Response of a 14-Story Anchorage, Alaska, Building in 2002 to Two Close Earthquakes and Two Distant Denali Fault Earthquakes

Mehmet Celebi,[a] **M.EERI**

The recorded responses of an Anchorage, Alaska, building during four significant earthquakes that occurred in 2002 are studied. Two earthquakes, including the 3 November 2002 M7.9 Denali fault earthquake, with epicenters approximately 275 km from the building, generated long trains of long-period ($>$1 s) surface waves. The other two smaller earthquakes occurred at subcrustal depths practically beneath Anchorage and produced higher frequency motions. These two pairs of earthquakes have different impacts on the response of the building. Higher modes are more pronounced in the building response during the smaller nearby events. The building responses indicate that the close-coupling of translational and torsional modes causes a significant beating effect. It is also possible that there is some resonance occurring due to the site frequency being close to the structural frequency. Identification of dynamic characteristics and behavior of buildings can provide important lessons for future earthquake-resistant designs and retrofit of existing buildings. [DOI: 10.1193/1.1779291]

INTRODUCTION

Station 8016 operated by National Strong Motion Program of the USGS is a fourteen-story, steel moment resisting framed building located in Anchorage, AK (coordinates 61.1922° N, 149.8645° W). The foundation of the building consists of single footings (without piles). The building appears geometrically symmetrical from outside. However, the locations of the elevators and stairwells are unsymmetrical in plan at different floors resulting in unsymmetrical distribution of stiffness and mass at different floors. The building seismic instrumentation and the associated free-field is schematically shown in Figure 1. The original analog 12-channel recorder and the accelerometers were deployed in 1989. The recorder was upgraded to a digital recording system before the events considered herein. The instrumentation scheme, at the time of the earthquake, deficient by today's practice, is now supplemented by a triaxial accelerometer in the basement as shown in Figure 1. The instrumentation was deployed to record responses of the building to seismic events and thus facilitate response studies to understand the behavior and assess the performance of the building during strong shaking events.

[a] U.S. Geological Survey, 345 Middlefield Rd., Menlo Park, CA 94025

Earthquake Spectra, Volume 20, No. 3, pages 693–706, August 2004;

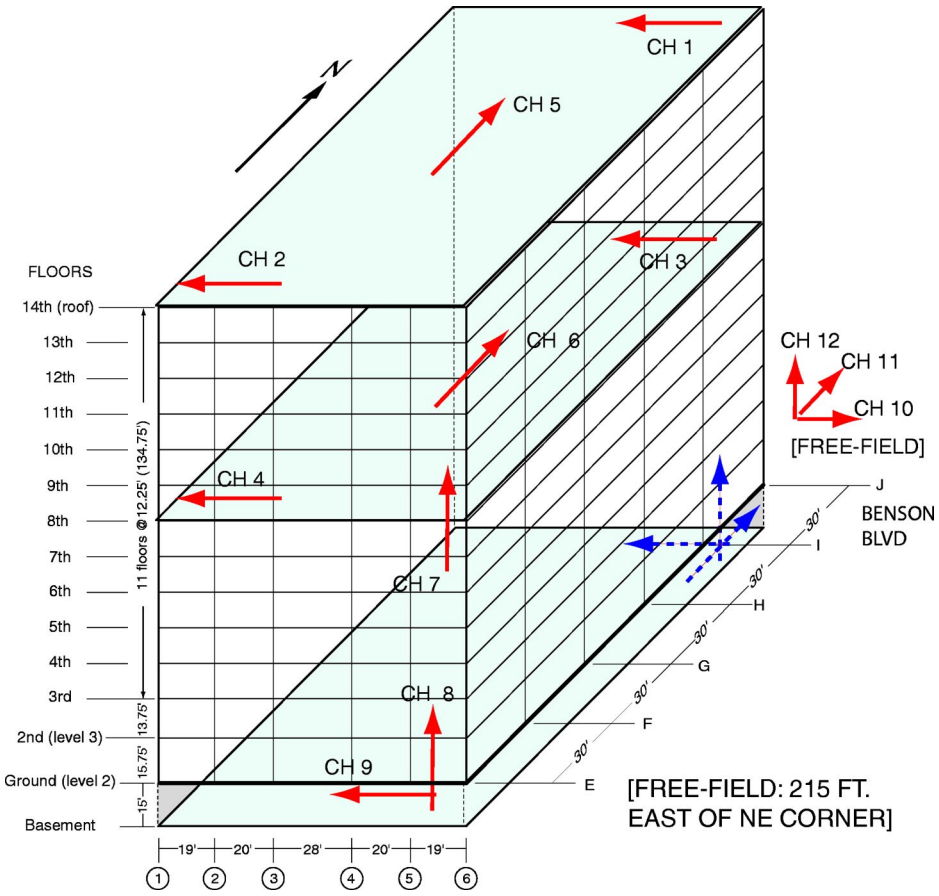

Figure 1. General schematic of the building with the sensors within the building and the free-field. The dashed tri-axial arrows indicate additional upgrade recently implemented for the instrumentation to provide motions of the building basement in the NS direction and additional motions in the vertical and EW directions.

FOUR EARTHQUAKES

During 2002, building responses were recorded during two pairs of earthquakes (Figure 2, Table 1; events 1 and 2, and events 3 and 4). Relative to Anchorage, Alaska, the epicenters of the four earthquakes are shown in Figure 2. The building response to each pair of earthquakes is different; hence, unique interpretations of the dynamic response characteristics of the building, in the specific geological and geotechnical environment in Anchorage, are required.

The 11-3-02 and 10-23-02 events (3 and 4) occurred on the Denali fault (Eberhart-Phillips et al. 2003) at shallow depths at distances $>$275 km from Anchorage and generated long trains of long-period ($>$1 s) surface waves in the Anchorage basin. On the other hand, the two smaller 2-6-02 earthquakes occurred along the subduction zone in-

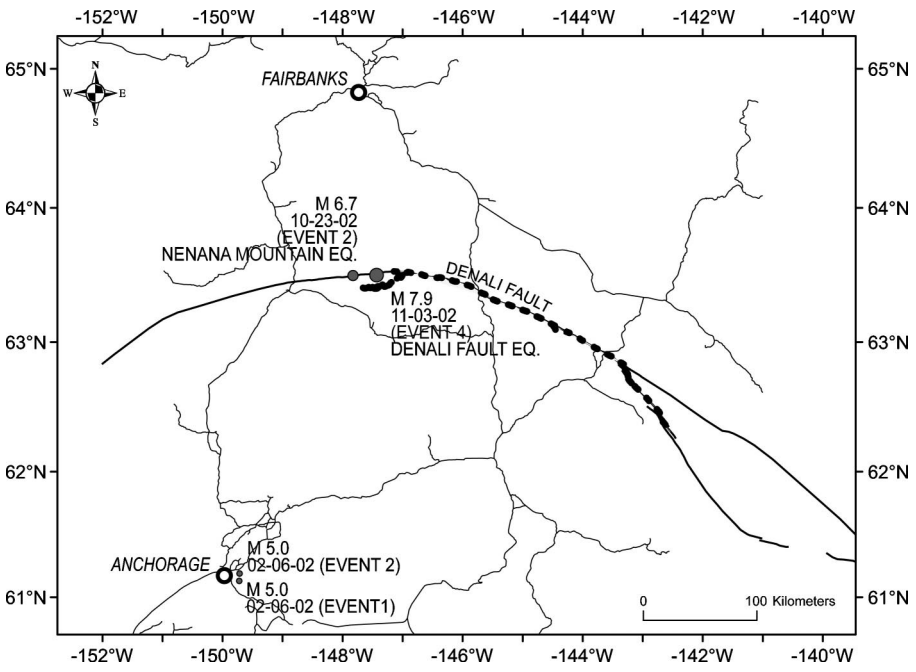

Figure 2. Locations of epicenters of four earthquakes relative to Anchorage, Alaska. Dashed line depicts the rupture during the 11-03-02 earthquake.

Table 1. Four events recorded in Anchorage (AK) Building

Event No Date	UTC	Magnitude	Lat. (N), Long. (W)	H (km)	D (km)
Event 1 02-06-02	17:18:46	Mb=4.9 (NEIC), ML=5.0	61.1684° 149.732°	37.7	7.6
Event 2 02-06-02	17:19:29	Mb=4.9 (NEIC) M=5.0	61.2076° 149.729°	36.6	7.5
Event 3 10-23-02	11:27	M6.7*	63.626° 148.016°	10	279
Event 4 11-03-02	22:12	M7.9	63.517° 147.525°	5	286

Notes

* All magnitudes in this paper, unless otherwise indicated, are moment magnitudes, M. Data compiled from nsmp.wr.usgs.gov.

H=depth

D=distance from building

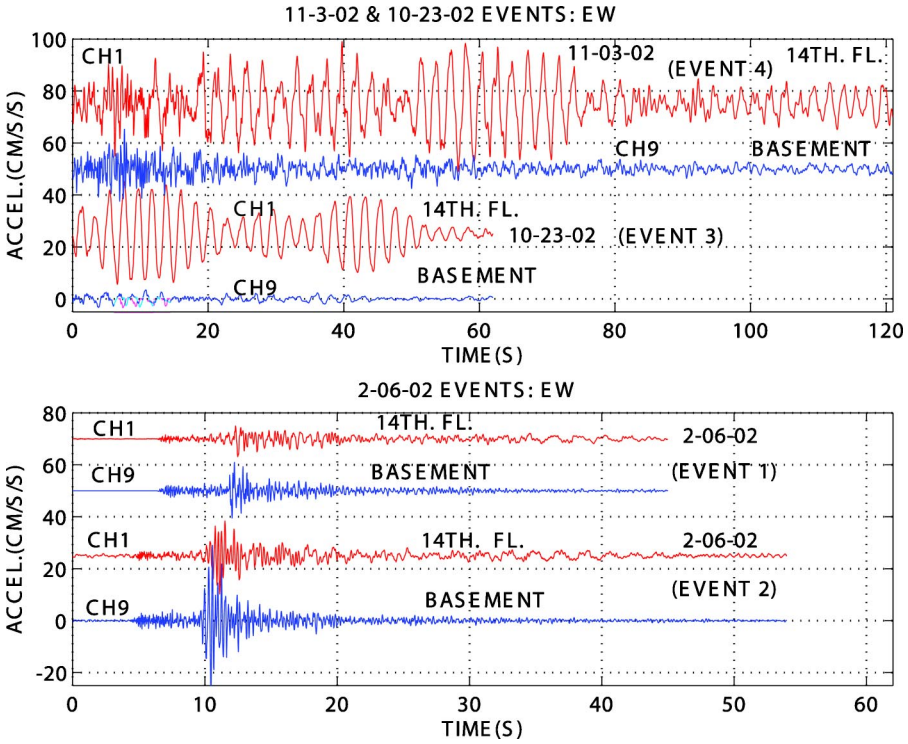

Figure 3. Recorded and equiscaled acceleration responses in the EW direction and at the 14th floor and the basement of the building during four earthquakes. Note different horizontal scales.

terface (at subcrustal depths) practically beneath Anchorage and produced higher frequency motions in Anchorage. Thus these two pairs of earthquakes have different tectonic settings, different frequency contents and as such their impacts on the response of the building in Anchorage are expected to be different.

During the four earthquakes, channel 3 (CH3 in Figure 1) malfunctioned. Furthermore, (a) lack of NS channel in the basement did not allow comparison of free-field motions with basement motions in the NS direction, and (b) lack of an additional vertical channel in the NW or SW corner of the basement did not allow reliable assessment of rocking motions, if any. Nonetheless, the existing data still provide ample means to analyze the response of the building.

ANALYSES OF RECORDED DATA

The recorded acceleration responses in the EW direction on the 14th floor and basement of the building during the four earthquakes are exhibited in Figure 3. Displacements computed from the recorded accelerations are provided in Figure 4. It is noted that the displacement time-histories of the 11-3-02 event have very long period (>30 second) pulse-like motion that appears both in the basement and 14th floor. This is

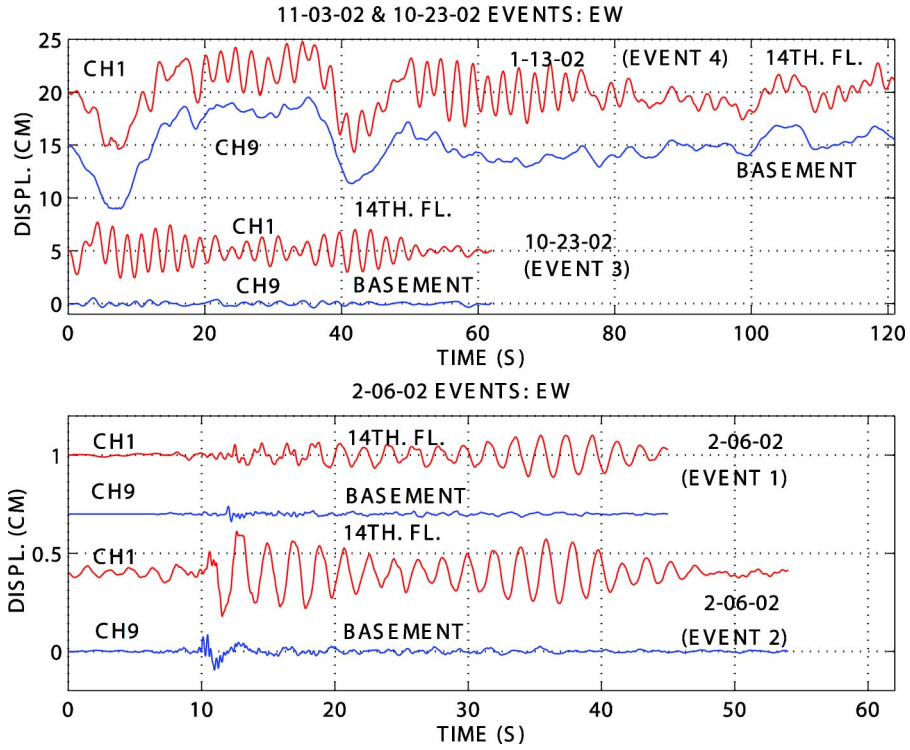

Figure 4. Equiscaled displacements computed from recorded acceleration responses in the EW direction and at the 14th floor and the basement of the building during four earthquakes. Note different horizontal scales.

caused by source effects and is explained by Frankel et al. (2002) and Eberhart-Phillips et al. (2003) as being due to occurrence of three sub-events. The building does not respond to this long-period motion. Essentially it rides along. On the other hand, the approximately 2-second vibrations that are seen in the 14th floor displacements are caused by the structural response.

BEATING EFFECT

Immediately noticeable from the building response is the beating effect clearly present in the acceleration data recorded at the roof (Figure 3) and the displacements computed from the acceleration data (Figure 4). Beating behavior is characterized by coupling between translational and torsional motions and low damping (Boroschek and Mahin 1991; Celebi 1994). Repetitively stored potential energy during the coupled translational and torsional deformations turns into repetitive vibrational energy. Thus periodic, repeating and resonating motions ensue as depicted in Figure 3. The beating becomes severe if the system is lightly damped. Therefore, first, the beating issue is investigated.

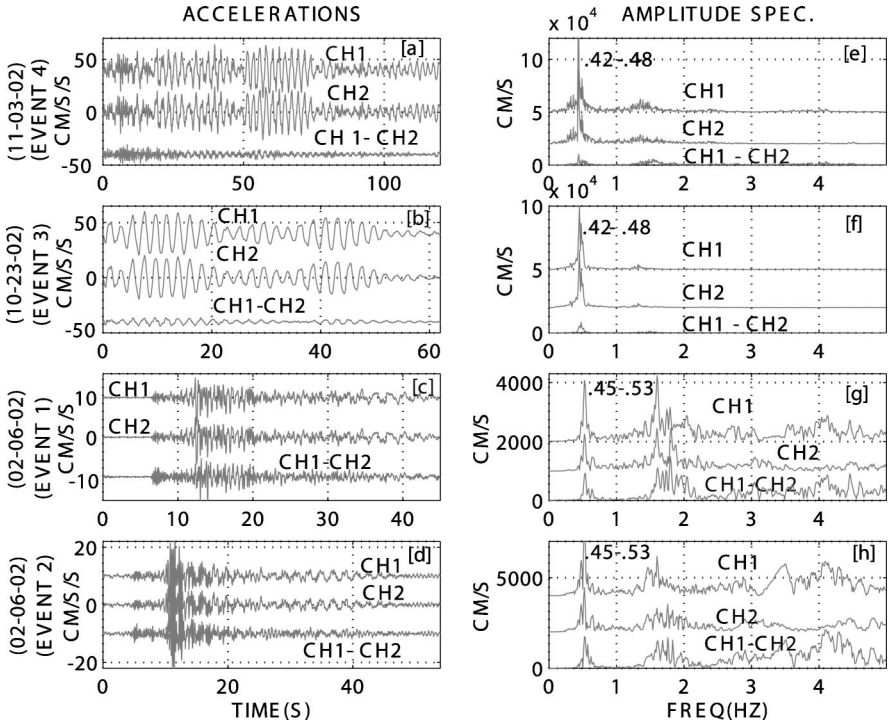

Figure 5. For each of the four events, (a-d) recorded (EW) translational and torsional accelerations at the roof and (e-h) their corresponding amplitude spectra. (Note the different horizontal time scales.) The order of events starts with larger structural response.

Figure 5 depicts for the four earthquakes and at the roof of the building, (a-d) the recorded (EW) translational and torsional accelerations and (e-h) their corresponding amplitude spectra. From these spectra, the first closely-coupled translational–torsional frequencies (periods) are identified to be within (a) 0.42–0.48 Hz (2.08–2.38 s) band for the 11-03-02 and 10-23-02 events, and (b) 0.45-0.53 Hz (1.89–2.22 s) band for the two 2-6-02 events. The lower frequency (higher period) within the ranges shown in Figure 5e-h is the translational frequency, f_2 (T_2), while the higher frequency is the torsional frequency, f_1 (T_1). Thus, the approximate beating period is computed for the 11-03-02 and 10-23-02 earthquakes as:

$$T_b = 2T_1T_2/(T_1-T_2) = 2(2.38)(2.08)/(2.38-2.08) = 33.0 \text{ s},$$

and for the February 6, 2002, earthquakes as:

$$T_b = 2T_1T_2/(T_1-T_2) = 2(1.89)(2.22)/(2.22-1.89) = 25.4 \text{ s}.$$

These computed beating periods are quite similar to those that can be visually identified in the acceleration response plots in Figures 3 and 5 and displacement plots in Figure 4.

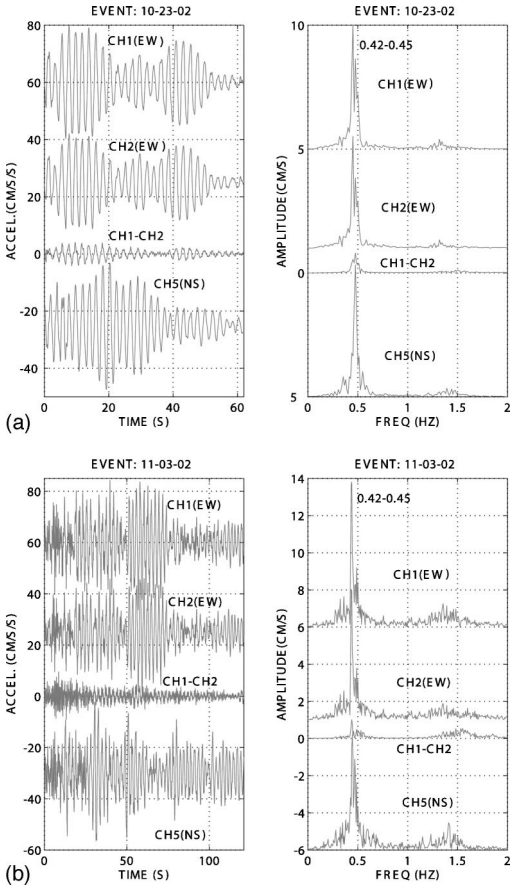

Figure 6. Comparison of the fundamental frequencies identified from amplitude spectra of EW (CH1 & CH2), NS (CH5) and torsional (CH1-CH2) accelerations recorded on the 14th floor during 10-23-02 (a) and 11-3-02 (b) events.

The energy of the higher modes at higher frequency than the fundamental frequency is more pronounced in events 1 and 2 as compared to 3 and 4. This may be attributed to the higher frequency content of the nearby earthquake motions of events 1 and 2 as compared to those of the distant events 3 and 4.

While the EW translational (CH1 and CH2) and torsional motions (CH1-CH2) have been considered thus far, the amplitude spectra of the NS accelerations (CH5) exhibit identical coupled translational-torsional frequencies. This is illustrated in Figure 6 where for both the 10-23-02 and 11-3-02 events, the amplitude spectra of accelerations at the 14th floor (CH1, CH2 in the EW direction, CH1-CH2 as torsional acceleration, and CH5 in the NS direction) bear identical fundamental frequencies. These are summarized in Table 2. Also noted in Figures 5 and 6 is the second coupled translational-torsional frequency at approximately 1.35 Hz.

Table 2. Identified dynamic characteristics

Event	Translational-Torsional Frequency (Period) Range Hz (second)	Damping ξ [%] System ID	Site Frequency (Period) Range Hz (second)
Event 1 02-06-02	0.45–0.53 (1.89–2.22)	3.3	0.30–0.36
Event 2 02-06-02	0.45–0.53 (1.89–2.22)	3.4	0.30–0.36
Event 3 11-03-02	0.42–0.48 (2.08–2.38)	3.9	0.30–0.36 (2.33–2.78)
Event 4 10-23-02	0.42–0.48 (2.08–2.38)	3.9	0.30–0.36

SYSTEM IDENTIFICATION

In Figure 7, we present a sample system identification analysis performed for November 3, 2002, event (event 4). The system identification analysis is performed using the ARX (acronym meaning autoregressive and X for extra input) model based on least squares method for single-input single-output (Ljung 1987) coded in commercially available system identification software (The Math Works 1995). One of the useful results of application of system identification procedures is the identification of modal damping percentages. These percentages for all four earthquakes are identified, to vary between 3.3–3.9% as summarized in Table 2. The lower damping percentages are determined from the data of the closer but lower shaking February earthquakes. On the other hand, the frequencies for the closely-coupled, translational-torsional structural frequencies are higher for the lower shaking February earthquakes; hence indicating nonlinear behavior depending on the level of shaking.

SITE-STRUCTURE RESONANCE

The reason why determination of site frequency is necessary is to infer possible resonation that can be caused by closeness of the site frequency to the structural frequency. It is possible to identify the site frequency of a building site by spectral analysis of the recorded responses of that building (Celebi 2003). In Figure 8a-d, for each of the four earthquakes, the amplitude spectra of CH1 (EW) at the roof and CH9 (EW) at the basement are plotted. In order to better identify the structural and site frequencies, these amplitude spectra are normalized and replotted in Figure 8e-h. While the dominance of structural frequencies is clearly observable (0.42-0.48 Hz for the 11-03-02 and 10-23-02 events and 0.45-0.53 Hz for the two 2-06-02 events), the frequencies within 0.30-0.36 band are also observable in the normalized amplitude spectra of basement response as well as that of the roof response. Thus, when spectral ratios are computed (Figure 8i-l), the ratios corresponding to the site response frequency are mostly around unity because, usually there is not much amplification of the site frequency at the roof level. That is, the amplitudes of the spectra of the roof and basement motions cancel out within the site

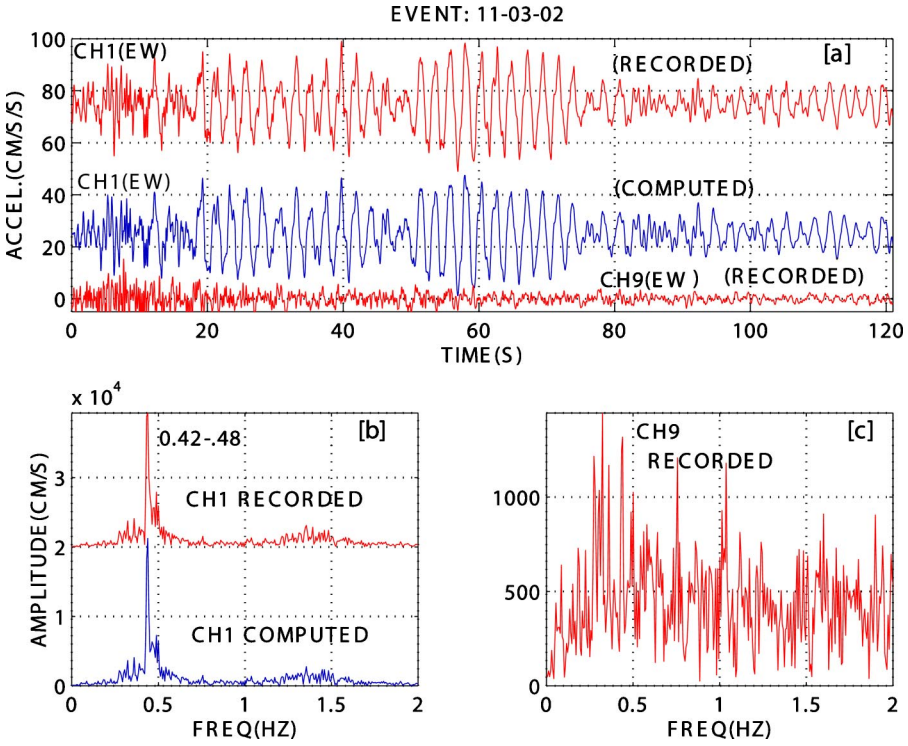

Figure 7. Sample system identification analysis. Results: (a) recorded input basement acceleration (CH9) and output roof acceleration (CH1) and computed output acceleration (CH9), (b) amplitude spectra of recorded and computed output accelerations (CH1) and (c) amplitude spectrum of input recorded accelerations (CH9).

frequency band. On the other hand, the structural frequency exhibits much larger spectral ratios (in this case >10) within the structural frequency bands. Therefore, it is safe to declare that the site frequency is most likely between 0.30-0.36 Hz band.

To further evaluate the site frequency, for the 11-03-02 event, we compute the spectral ratio of the amplitude spectra of the recorded horizontal to vertical accelerations at the free-field site of the building (Figure 1) and also at another free-field site (station 8024) that is located within 1.5 km to the south-west of the building. In absence of stiff-soil or rock motions, at alluvial sites, the ratios of amplitude spectra of horizontal to vertical motions provide a means to assess transfer functions (Nakamura 1989, 2000). For the building associated free-field site, Figure 9 shows (a) acceleration time-histories of the three components at the free-field, (b) their corresponding amplitude spectra and (c) ratios of amplitude spectra of horizontal to vertical accelerations. Thus it is seen from the site transfer functions (ratios) that clearly there is a site frequency within 0.30-0.36 Hz band. The lower frequency peaks, at around 0.1 Hz, are attributed to source effect appearing as horizontally polarized shear (SH) waves (Boore 2002). Similarly, Figure 10

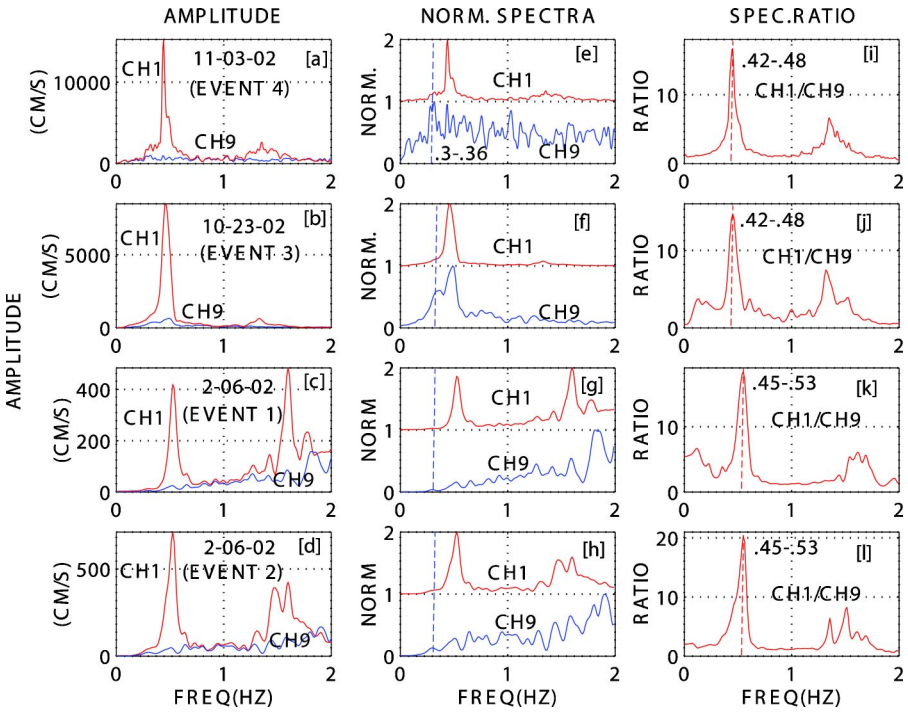

Figure 8. For each of the four earthquakes, (a-d) amplitude spectra of CH1 (EW) at the roof and CH9 (EW) at the basement, (e-h) normalized amplitude spectra of the same, and (i-l) spectral ratios. Site frequency (0.3–0.36 Hz) in the normalized spectra is noted but disappears in the spectral ratio plots. The order of events starts with larger structural response.

depicts the acceleration time-histories, amplitude spectra and ratios for free-field station 8024. Again, while the site frequency band of 0.30-0.36 Hz is observable, a similar source-caused frequency around 0.1 Hz is observed.

For sake of simplicity, we take the average site frequency as 0.33 Hz, and the average structural frequency as 0.45 Hz for the 11-3-02 and 10-23-02 events and 0.49 Hz for the 2-6-02 events. Thus, for any resonance to occur, the amplification (A) of a damped system (with damping ratio, ξ) can be computed by:

$$A = 1/[(1-r^2)^2+(2\xi r)^2]^{0.5}$$

where r is the ratio of site frequency to the structure frequency. Therefore, for r $=0.33/0.45$ or $0.33/0.49$ ($r=0.674–0.733$) and $\xi \approx .035$, the expected amplification $A \approx 1.83$-2.15. It can be concluded that, while this is not a strong resonating situation, nevertheless, limited resonance does occur at this site.

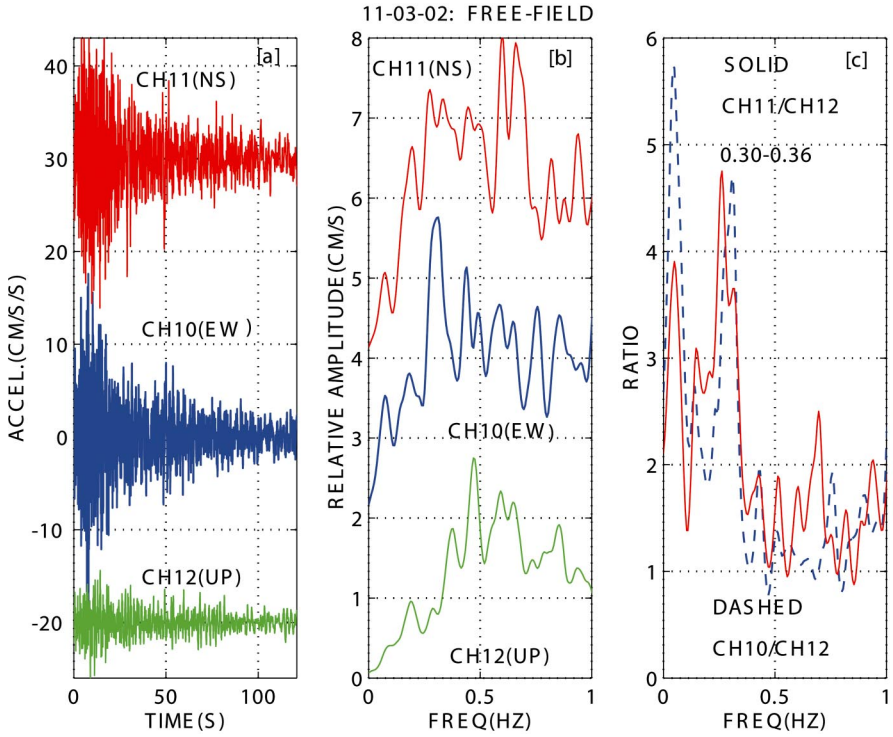

Figure 9. For the 11-3-02 event, (a) acceleration time-histories of the building associated free-field site, (b) corresponding amplitude spectra and (c) ratios of amplitude spectra of horizontal to vertical accelerations depicting site frequency band 0.3–0.36 Hz. Lower frequency peak at around 0.1 Hz is attributed to source effects.

AVERAGE DRIFT RATIOS

As can be expected, the small displacement responses computed from accelerations do not result in significant drift ratios. As seen in Figure 11, the largest relative displacement between the 14th floor and the basement is $<$5 cm. The height of the building without the basement is 164.25 ft. ($\sim$50 m). Thus, an average drift ratio of 5/5000 $=$1/1000$=$0.1% is obtained. Normally, this level of drift ratio is well below damage level.

CONCLUSIONS:

The building response data indicate the following.

1. The input motions affecting the response of the building during the 2-6-02 events (events 1 and 2) have higher frequency content as compared to the later events (events 3 and 4). Thus, the impact on the building response is less and are less prone to cause building resonance. However, amplitude spectra of all

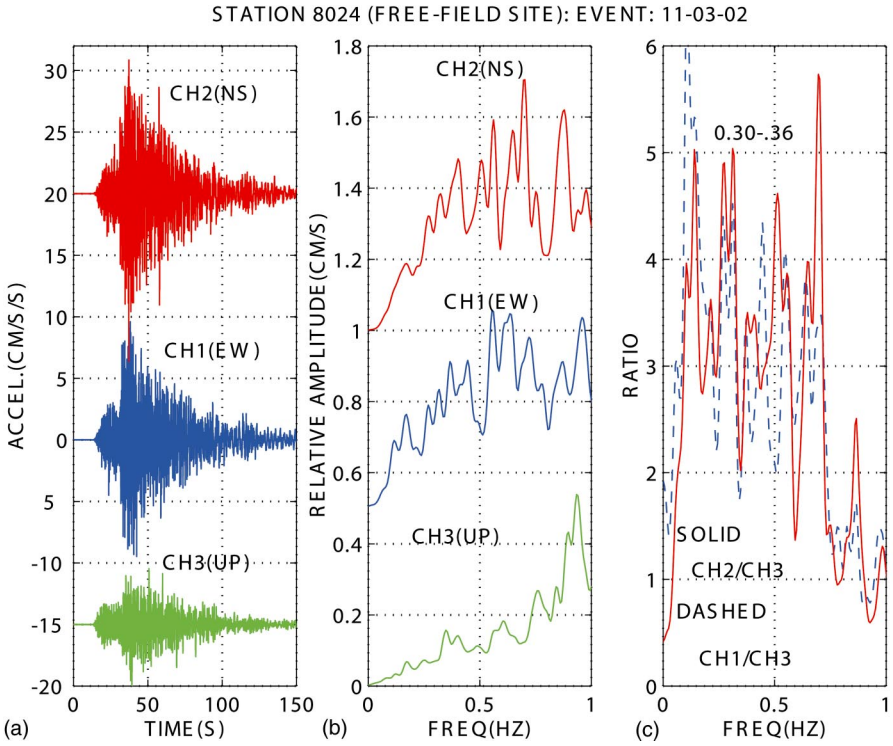

Figure 10. For the 11-3-02 event, (a) acceleration time-histories of free-field site (station 8024) located approximately 1.5 km from the building, (b) corresponding amplitude spectra and (c) ratios of amplitude spectra of horizontal to vertical accelerations depicting site frequency band 0.3–0.36 Hz. Lower frequency peak at around 0.1 Hz is attributed to source effects.

events show that higher modes are considerably more pronounced in the response of the building during the nearby events (1 and 2) due to higher frequency content.

2. Translational and torsional frequencies are closely coupled but are also changing according to the shaking level and frequency content of the input motions caused by the four earthquakes. The building was not damaged and therefore it can be inferred that the nonlinearity in the structural frequency can be attributed to interaction of the building with the site.
3. Close-coupling of translational and torsional modes causes significant beating effect.
4. System identification techniques are used to extract critical damping ratios of 0.033-0.039 which also indicates nonlinearity due to level of shaking. The higher the shaking, the higher the damping.
5. Site resonant frequency between 0.30–0.36 Hz is identifiable from the re-

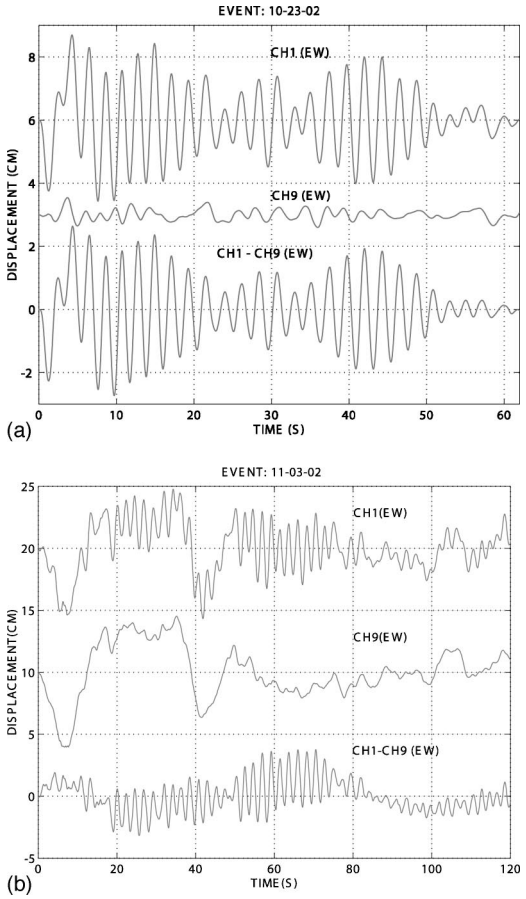

Figure 11. Displacement time-histories at, and relative displacement time-histories between, the 14th floor and the basement of the building for the 10-23-02 (a) and 11-03-02 (b) events. The relative displacements are used to compute average drift ratios.

corded responses of the building and free-field sites. The site frequency is close enough to the structural frequency to cause limited resonating amplification of building response motions.

6. Average drift ratios from the earthquakes are not significant to indicate and unlikely to have caused any damage.
7. The building instrumentation during the four earthquakes was deficient and is now improved by adding a tri-axial accelerometer in the NE corner of the building. This addition will provide better assessment of (a) rocking motions of the building, if any, (b) the NS channel of the tri-axial accelerometer in the basement will allow comparison of the free-field motion with that of the basement motion as it is influenced by structural vibration and serve as a basis for input motions in the NS direction during analysis, and (c) the EW component

of the tri-axial accelerometer will enable assessment of differential EW motions of the basement, if any. Finally, in the future, it will be important to add at least two orthogonal horizontal channels to the ceiling of the basement to allow assessment of variation of the basement motions with that of the ground floor motions–particularly for this building, which has shallow foundations that consist of individual footings without piles.

REFERENCES

Boore, D., 2002. Personal communication.

Boroschek, R. L. and Mahin, S. A., 1991. *Investigation of the seismic response of a lightly-damped torsionally-coupled building*, Univ. of California, Berkeley, Earthquake Engineering Research Center Report UCB/EERC-91/18, 291 pp.

Celebi, M., 1994. Response study of a flexible building using three earthquake records, *Proc. ASCE Structures Congress XII*, Atlanta, Georgia, **2**, American Society of Civil Engineers, 1220–1225.

Celebi, M., 2003. Identification of site frequencies from building records, *Earthquake Spectra* **19** (1), 1–23.

Eberhart-Phillips, D., Haeussler, P. J., Freymueller, J. T., Frankel, A. D., Rubin, C. D., Craw, P., Ratchkovski, N. A., Anderson, G., Crone, A. J., Dawson, T. E., Fletcher, H., Hansen, R., Harp, E. L., Harris, R. A., Hill, D. P., Hreinsdóttir, S., Jibson, R. W., Jones, L. M., Keefer, D. K., Larsen, C. F., Moran, S. C., Personius, S. F., Plafker, G., Sherrod, B., Sieh, K., and Wallace, W. K., 2003. The 2002 Denali fault earthquake, Alaska: a large magnitude, slip-partitioned event, *Science* **300**, 1113–1118.

Frankel, A. D., Biswas, N. N., Martirosyan, A. H., Dutta, U., and McNamara, D. E., 2002. Rupture process of the M7.0 Denali fault, Alaska, earthquake determined from strong-motion recordings, Abstract S72F-1340, *Proc., AGU Fall Meeting*, San Francisco, California, 6–10, Dec. 2002.

Ljung, L., 1987. *System Identification–Theory for the User*, Prentice-Hall, 1987, 519 p.

Nakamura, Y., 1989. A method for dynamic characteristics estimation of subsurface using microtremor on the ground surface, *QR of RTRI* **30** (1) 25–33.

Nakamura, Y., 2000. Clear identification of fundamental idea of Nakamura's technique and its applications, CD-ROM *Proceedings, 12th World Conference on Earthquake Engineering*, Auckland, New Zealand.

The Math Works, 1995 edition. *User's Guide: Identification Toolbox for use with Matlab*, The MathWorks, South Natick, Mass., 200 p.

(Received 1 December 2003; accepted 27 January 2004)